U–Pb geochronology of Cretaceous magmatism on Svalbard and Franz Josef Land, Barents Sea Large Igneous Province

Article *in* Geological Magazine · November 2013

DOI: 10.1017/S0016756813000162

CITATIONS
94

READS
868

7 authors, including:

S. Polteau
SurfExGeo
62 PUBLICATIONS **1,062** CITATIONS
SEE PROFILE

Sverre Planke
Volcanic Basin Petroleum Research; CEED University of Oslo
317 PUBLICATIONS **8,506** CITATIONS
SEE PROFILE

Jan Inge Faleide
University of Oslo
387 PUBLICATIONS **8,984** CITATIONS
SEE PROFILE

Henrik Hovland Svensen
University of Oslo
186 PUBLICATIONS **5,683** CITATIONS
SEE PROFILE

Geol. Mag. **150** (*6*), *2013, pp. 1127–1135. © Cambridge University Press 2013*
doi:10.1017/S0016756813000162

U–Pb geochronology of Cretaceous magmatism on Svalbard and Franz Josef Land, Barents Sea Large Igneous Province

FERNANDO CORFU*†, STÉPHANE POLTEAU‡, SVERRE PLANKE‡, JAN INGE FALEIDE*, HENRIK SVENSEN§, ANDREW ZAYONCHECK¶‖ & NIKOLAY STOLBOV‖

*Department of Geosciences, University of Oslo, Postbox 1047 Blindern, N-0316 Oslo, Norway
‡Volcanic Basin Petroleum Research AS, Forskningsparken, Gaustadalléen 21, N-0349 Oslo, Norway
§Physics of Geological Processes, University of Oslo, Postbox 1048 Blindern, N-0316 Oslo, Norway
¶Geological Institute of the Russian Academy of Science, St Petersburg Laboratory, 190121, 120 Moyka Quay, St Petersburg, Russia
‖All-Russian Research Institute for Geology and Mineral Resources of the World Ocean 190121, 1 Angliysky Avenue, St Petersburg, Russia

(*Received* 14 June 2012; *accepted* 1 February 2013; *first published online* 11 June 2013)

Abstract – The opening of the Arctic oceanic basins in the Mesozoic and Cenozoic proceeded in steps, with episodes of magmatism and sedimentation marking specific stages in this development. In addition to the stratigraphic record provided by sediments and fossils, the intrusive and extrusive rocks yield important information on this evolution. This study has determined the ages of mafic sills and a felsic tuff in Svalbard and Franz Josef Land using the isotope dilution thermal ionization mass spectrometry (ID-TIMS) U–Pb method on zircon, baddeleyite, titanite and rutile. The results indicate crystallization of the Diabasodden sill at 124.5 ± 0.2 Ma and the Linnévatn sill at 124.7 ± 0.3 Ma, the latter also containing slightly younger secondary titanite with an age of 123.9 ± 0.3 Ma. A bentonite in the Helvetiafjellet Formation, also on Svalbard, has an age of 123.3 ± 0.2 Ma. Zircon in mafic sills intersected by drill cores in Franz Josef Land indicate an age of 122.7 Ma for a thick sill on Severnaya Island and a single grain age of ≥122.2 ± 1.1 Ma for a thinner sill on Nagurskaya Island. These data emphasize the importance and relatively short-lived nature of the Cretaceous magmatic event in the region.

Keywords: baddeleyite, Cretaceous, Franz Josef Land, mafic sills, Svalbard.

1. Introduction

During the Mesozoic and Cenozoic, the high Arctic (Fig. 1) underwent multiple stages of rifting, sedimentation and magmatism in connection with the opening of the Atlantic and Arctic oceans. Cretaceous magmatic activity is considered to have been one of the main stages in this evolution and to have resulted in the High Arctic Large Igneous Province, termed HALIP (Maher, 2001; Buchan & Ernst, 2006; Minakov *et al.* 2012), extending from the Canadian Arctic Archipelago to Franz Josef Land. The mafic extrusive and intrusive rocks found in the Barents Sea define the Barents Sea Large Igneous Province (BLIP), and are an important component of the HALIP. The duration of this magmatic event and its influence on the tectonic evolution of the region remain uncertain however (e.g. Alvey *et al*. 2008). Ernst & Bleeker (2010) suggested that HALIP was emplaced during two phases at 130 and 90 Ma, coinciding with the opening of the Arctic Ocean. Much younger activity between 70 and 60 Ma is known to have built the Kap Washington volcanic succession at the northern edge of Greenland (Thorarinsson *et al*. 2011) while magmatism at 55 Ma (Charles *et al*. 2011) signals the break-up of the North Atlantic and Arctic Oceans.

On Franz Josef Land, basalts related to the HALIP are intercalated with fossiliferous sedimentary strata assigned from the Hauterivian to the Albian (*c.* 136–100 Ma) (Amundsen *et al*. 1998) but such basalts also yield K–Ar dates that vary greatly, the majority of them from 175 to 92 Ma but with a peak at about 123 Ma (Piskarev *et al*. 2009). Radiometric K–Ar determinations for mafic sills (Tarakhovsky *et al*. 1983; Dibner, 1998) provided a range of ages from the Permian (288 ± 20 Ma) to the Oligocene (34 ± 2 Ma) although more recent K–Ar studies of 14 samples from the wells and 8 from outcrops indicate a much shorter period of activity with ages of 131–108 Ma, averaging 116 ± 5 Ma (Grachev *et al*. 2001); the short timespan is comparable to that of the Siberian traps where magmatic activity did not last more than 2–3 Ma (Grachev, 2000).

The broad distribution of K–Ar and Ar–Ar dates from Svalbard and Franz Josef Land allows the interpretation that the magmatic evolution in the Arctic could have been a protracted series of events. For example, the compilation of Maher (2001) could be interpreted as indicating almost 150 Ma of oscillating,

†Author for correspondence: fernando.corfu@geo.uio.no

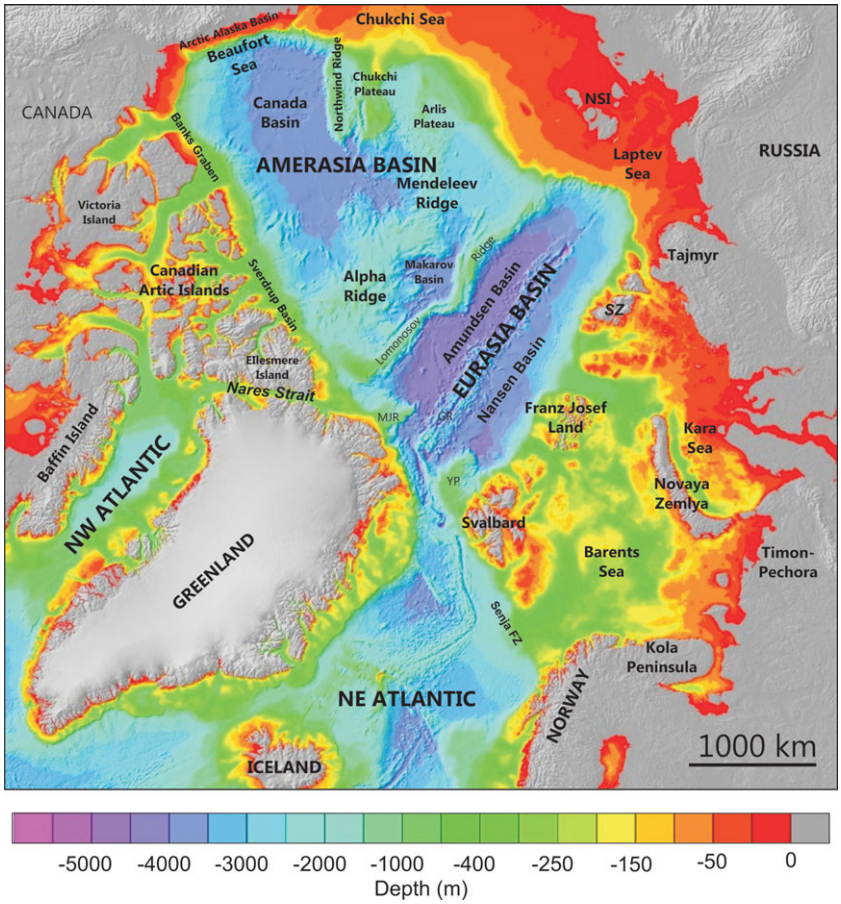

Figure 1. Bathymetric map showing the position of Svalbard and Franz Josef Land at the edge of the Barents Sea platform and in relation to the other basins of the Arctic realm. Abbreviations: FZ – fault zone; GR – Gakkel Ridge; MJR – Morris Jesup Rise; NSI – New Siberian Islands; YP – Yermak Plateau.

but essentially uninterrupted magmatic activity (see also Levskii *et al*. 2006; Nejbert *et al*. 2011). Age variations observed between samples of common units (Nejbert *et al*. 2011) suggest, however, that some of the dates record secondary resetting processes. Obtaining a reliable record for the timing of magmatism within this province is crucial for correlating the variety of magmatic expressions in the Arctic, for understanding the processes that caused their formation and for verifying whether their emplacement can be linked to some extreme climatic upheavals registered in the sedimentary record. Use of the more robust U–Pb method can help to consolidate the chronological record; in this paper we therefore report isotope dilution thermal ionization mass spectrometry (ID-TIMS) U–Pb ages for chemically abraded zircon from (1) a Cretaceous felsic tuff in Svalbard; (2) zircon, rutile and titanite from two mafic sills in Svalbard; and (3) zircon and baddeleyite from four drill cores intersecting mafic sills in Franz Josef Land. The felsic tuff occurs in the Helvetiafjellet Formation below the anoxic level, which is characterized by a negative $\delta^{13}C$ excursion at the boundary between Barremian and Aptian. The sample therefore provides the means to date the volcanic event and constrain the age of the Barremian–Aptian boundary.

2. Geological setting

The archipelagos of Svalbard and Franz Josef Land are situated on continental crust close to the northern edge of the Barents Sea platform (Fig. 1; Faleide *et al*. 2008). The crust underneath Svalbard comprises largely Precambrian rocks reworked during the Caledonian orogeny and is locally overlain by post-orogenic Devonian sedimentary deposits (Harland *et al*. 1997).

The post-Devonian evolution started with Permo-Carboniferous rifting and the development of discrete NE-trending troughs, mainly in the Barents Sea, followed by formation of an extensive post-rift carbonate platform with local accumulations of evaporitic sequences (Worsley, 2008). The Triassic is characterized by a decrease in subsidence, while the Jurassic–Cretaceous transition was dominated by the deposition of fine clastic sedimentary rocks. The Early Cretaceous was characterized by crustal uplift in the north, apparently related to the arrival of a mantle plume which was later responsible for HALIP volcanism. This regional doming resulted in deltaic progradation over the base Cretaceous unconformity. The northern uplift continued into the Aptian–Albian and through the Late Cretaceous (Worsely, 2008). These events preceded the Cenozoic break-up

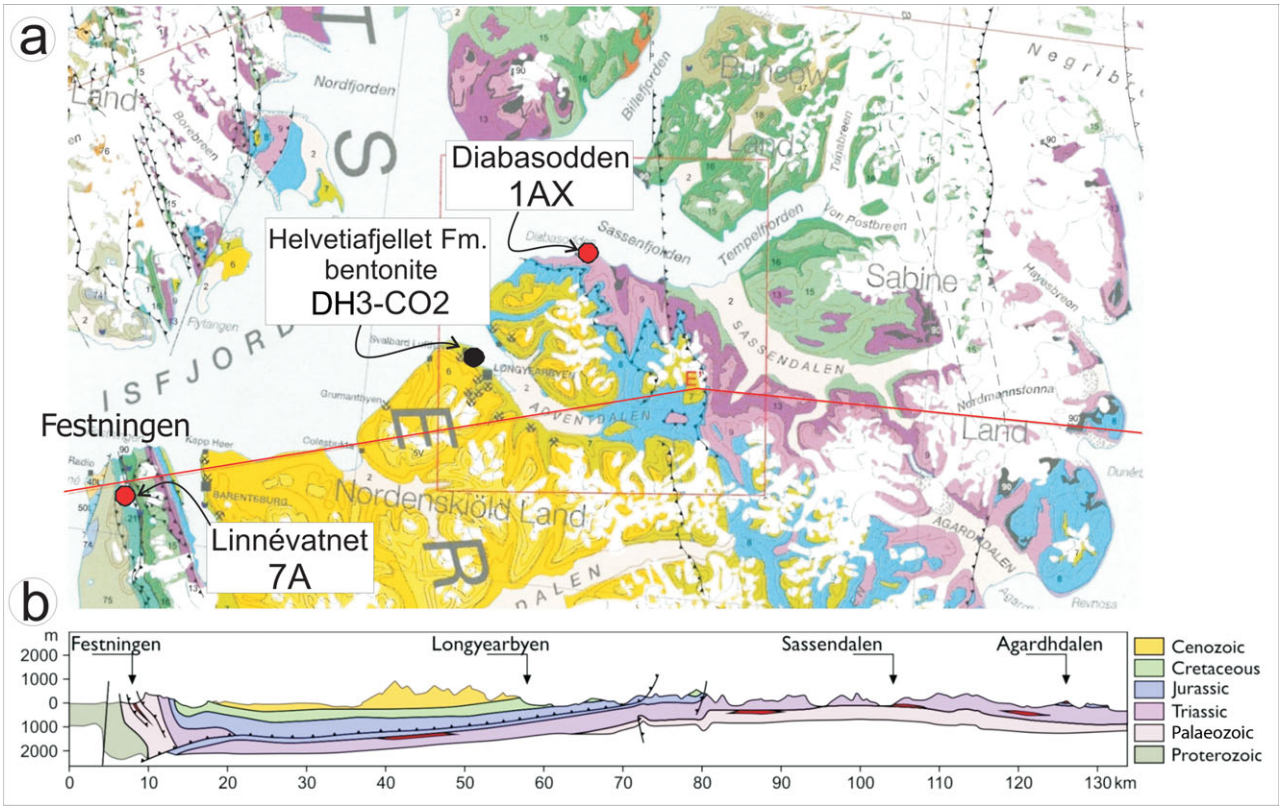

Figure 2. (a) Geological map of the region around Isfjorden, western Svalbard. (b) Inset with a cross-section illustrating the stratigraphic and tectonic relationships and showing the sample locations.

of Laurasia, which resulted in the opening of the Norwegian–Greenland Sea and the Eurasia Basin. These domains were linked across a SE-trending megashear system which involved both transtensional and transpressional components, the latter reflected in the development of the Spitsbergen Fold-and-Thrust Belt (Faleide *et al*. 2008). The regional variations resulted in variable stratigraphic developments between Svalbard and Franz Josef Land, the latter exhibiting both a much thicker Triassic sequence (4200 v. 1000 m) and much more abundant Cretaceous mafic sills and flows (Solheim *et al*. 1998).

The basaltic lava on Kong Karls Land and Franz Josef Land was preferentially extruded in synclines correlated to the Helvetiafjellet Formation, providing stratigraphic evidence of Early Cretaceous volcanic activity in the region. A geochemical study of basalts from Franz Josef Land shows that they are tholeiitic, and have positive εNd values (+6 to +4) indicative of a provenance from depleted mantle, but with more elevated Sr initial values suggestive of seawater contamination (Amundsen *et al*. 1998). The mafic sill complexes were emplaced preferentially in organic-rich sedimentary sequences, such as the Jurassic Agardhfjellet Formation and in the Triassic and Permian (Grogan *et al*. 2000).

3. Samples

The Svalbard samples were collected during a sampling campaign in April 2010 along a transect from Isfjorden Radio to Agardhbukta. All samples were taken from the coarser portions of thick (30–50 m) mafic sills. Sample 1AX represents the Diabasodden sill intruding Triassic strata at Diabasodden, and the other (sample 7A) occurs in Palaeozoic strata in an upturned section at Festingen, Linnévatnet (Fig. 2). The latter sample is highly altered with plagioclase entirely saussuritized, whereas pyroxene is for the most part still well preserved. Long skeletal ilmenite is only locally altered. The alteration assemblage comprises biotite, iddingsite, chlorite, sericite, chlorite, calcite and epidote, in addition to a green amphibole forming locally from pyroxene. Rutile appears to be associated with the breakdown of pyroxene, but the association of titanite within this secondary assemblage is uncertain.

A third sample is a felsic tuff intersected by the DH3 borehole near Longyearbyen, drilled to test the site as a potential repository for CO_2. The core was sampled at the University Centre of Svalbard, Longyearbyen. In the boreholes the Barremian – early Aptian Helvetiafjellet Formation is overlain by early Aptian sapropel-rich shales of the Carolinefjellet Formation.

A suite of samples was also obtained from drill cores in Franz Josef Land. In 1976–1981 three deep stratigraphic wells were drilled on the islands of Alexandra (Nagurskaya well), Graham Bell (Severnaya well) and Heyes (Heyes well) (Fig. 3). All three wells penetrate 3–87 m thick basaltic sheets, most of them sills but several dykes were also met in the Nagurskaya well. The thick sills intrude Late Triassic (Carnian) sequences (Dypvik *et al*. 1998; Piskarev *et al*. 2009).

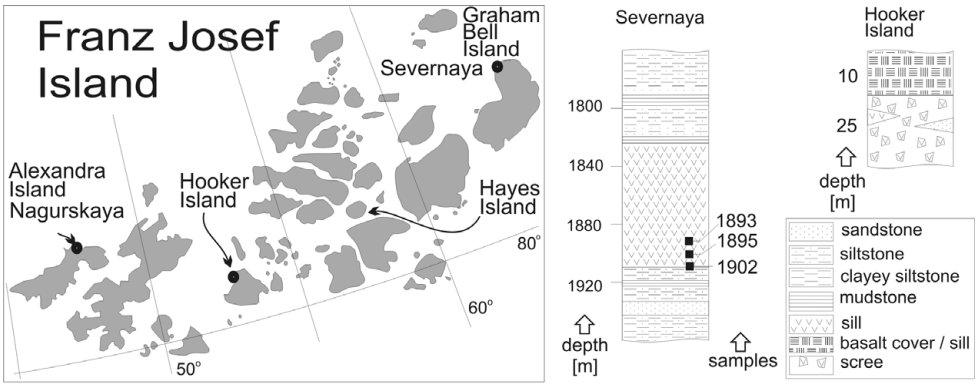

Figure 3. Map of Franz Josef Land with sampled drill hole sites. The sections on the right side of the figure illustrate the stratigraphic context of the samples from Severnaya and Hooker Island. The section of the Nagurskaya well is characterized by many sills only a few metres thick and is not shown.

Three of the samples (1893, 1895, 1902) represent gabbro-doleritic domains at the bottom of the 87 m thick sill in the Severnaya well. In addition we also processed a sample from a sill or basalt layer on Hooker Island (FJL 03/07), but could not find datable magmatic accessories. Similarly, an attempt to separate zircon and/or baddeleyite from a sill drilled by the Ludlow well in the Eastern Barents Sea was not successful.

4. U–Pb geochronology

4.a. Analytical procedure

The samples from Svalbard were crushed and processed through a combination of Wilfley table, heavy liquid separation and magnetic separation; only two of eight mafic sill samples yielded zircon. We also obtained mineral separates from several mafic sills from the Severnaya, Nagurskaya and Hooker Island boreholes on Franz Josef Land. After selection under a binocular microscope, the zircons were chemically abraded (Mattinson, 2010), a technique that involves annealing for three days at 900 °C followed by partial dissolution in HF for one night at *c.* 190 °C. Baddeleyite, rutile and titanite were not abraded. Zircon, baddeleyite and rutile were dissolved in bombs at *c.* 190 °C and titanite in Savillex vials on a hotplate, all of them after addition of a ^{202}Pb–^{205}Pb–^{235}U spike. The rest of the procedure, based on Krogh (1973), is as described in Corfu (2004). The data have been corrected for ^{230}Th disequilibrium following Schärer (1984), assuming a Th/U ratio in the magma of 4. The correction increases the ^{206}Pb/^{238}U age by about 0.1 Ma for the samples with the lowest Th/U, but is next to irrelevant for some of the zircons with high Th/U. Blank correction was $\leq$2 pg Pb and 0.1 pg U. However, a higher blank likely affected some of the baddeleyite analyses due to the difficulty in transferring the very tiny blades into the dissolution vessel. For most zircon analyses, all common Pb can be attributed to blank and the occasional excesses were corrected using the model of Stacey & Kramers (1975). Common Pb in rutile and titanite was corrected using the composition of coexisting pyroxene (Table 1). Decay constants are those of Jaffey *et al*. (1971). Plotting and calculations were performed with the program Isoplot of Ludwig (2009). All the age uncertainties represent 2σ and were calculated by propagating all sources of analytical error, but do not include spike or decay constant uncertainties.

4.b. Sample 1AX: Diabasodden sill, Svalbard

The sample yielded a very coherent set of zircon crystals having the classical appearance of zircon in rapidly crystallized mafic magmas, that is, long euhedral prisms with prominent {100} and {101} crystal faces, almost ubiquitous longitudinal cavities either with melt or empty, and generally rusty. The analysed grains show high U contents and high Th/U and yield four overlapping analyses, which define a weighted mean ^{206}Pb/^{238}U age of 124.5 ± 0.2 Ma (Fig. 4a; Table 1).

4.c. Sample 7A: Linnévatnet sill, Svalbard

The zircon population in this sample was of the same general morphological type as in sample 1AX, but with fewer and less well-preserved crystals. The analyses are spread along the concordia curve (Fig. 4b), suggesting that some of the grains likely contained xenocrystic components. The three youngest zircon data points yield a weighted mean ^{206}Pb/^{238}U age of 124.7 ± 0.3 Ma. Rutile occurs as orange-red crystals, translucent and in most cases altered. The two analyses indicate U contents of about 10 ppm and yield data that overlap the youngest zircon data, indicating formation in late stages of essentially the same process. Titanite forms clear euhedral to anhedral crystals containing the same amount of U but more Th than the rutile. The two analyses yield an age of 123.9 ± 0.3 Ma, younger than zircon and rutile and likely reflecting post-magmatic alteration processes.

Table 1. U–Pb data

Characteristics[a]	Weight (μg)	U (ppm)	Th/U[b]	Pbc[c] (pg)	$^{206}Pb/^{204}Pb$[d]	$^{207}Pb/^{235}U$[e]	±2σ (abs)	$^{206}Pb/^{238}U$[e]	±2σ (abs)	ρ	$^{207}Pb/^{206}Pb$[e]	±2σ (abs)	$^{206}Pb/^{238}U$[e] (age in Ma)	±2σ	$^{207}Pb/^{235}U$[e] (age in Ma)	±2σ
1AX (SV10HS-1AX), Diabasodden mafic sill, Svalbard 78.3592, 16.1656																
Z eu lp CA [3]	<1	>820	1.34	2.9	370.8	0.1318	0.0022	0.019629	0.000099	0.45	0.0487	0.0007	125.3	0.6	125.7	2.0
Z eu lp CA [4]	1	2190	1.42	0.6	4146	0.1309	0.0009	0.019527	0.000119	0.92	0.0486	0.0001	124.7	0.8	124.9	0.8
Z eu lp CA [3]	<1	>960	1.71	0.7	1679	0.1309	0.0008	0.019489	0.000068	0.67	0.0487	0.0002	124.4	0.4	124.9	0.7
Z eu lp CA [10]	3	980	1.92	2.0	1846	0.1308	0.0007	0.019484	0.000049	0.61	0.0487	0.0002	124.4	0.3	124.8	0.7
7A (SV10HS-7A), coarse pegmatitic portion of mafic sill, Linnevatnet, Svalbard 78.03374, 13.88448																
Z eu lp CA [1]	<1	>530	2.80	1.9	363.8	0.1361	0.0031	0.020155	0.000081	0.45	0.0490	0.0010	128.6	0.5	129.6	2.7
Z eu lp CA [1]	<1	>230	1.37	1.4	220.2	0.1393	0.0051	0.019791	0.000067	0.61	0.0511	0.0018	126.3	0.4	132.4	4.6
Z eu lp CA [1]	1	350	1.98	0.6	705.5	0.1334	0.0017	0.019755	0.000057	0.46	0.0490	0.0006	126.1	0.4	127.1	1.5
Z eu lp CA [1]	1	600	1.75	2.2	347.7	0.1318	0.0028	0.019576	0.000073	0.45	0.0488	0.0010	125.0	0.5	125.7	2.5
Z eu lp CA [1]	1	230	1.22	0.5	554.2	0.1320	0.0023	0.019514	0.000079	0.45	0.0491	0.0008	124.6	0.5	125.9	2.1
Z eu lp CA [1]	1	410	2.42	1.1	463.7	0.1305	0.0024	0.019440	0.000102	0.44	0.0487	0.0008	124.1	0.6	124.5	2.2
R eu–an NA [37]	29	10	0.07	6.9	67.9	0.1325	0.0073	0.019657	0.000091	0.67	0.0489	0.0025	125.5	0.6	126.4	6.5
R eu–an NA [24]	20	9	0.15	6.7	52.0	0.1323	0.0107	0.019492	0.000114	0.73	0.0492	0.0038	124.4	0.7	126.1	9.5
T eu–an NA [50]	59	11	0.46	9.2	104.2	0.1304	0.0036	0.019428	0.000065	0.58	0.0487	0.0013	124.0	0.4	124.5	3.3
T eu–an NA [40]	42	10	0.50	16.9	48.8	0.1303	0.0061	0.019391	0.000067	0.55	0.0487	0.0022	123.8	0.4	124.3	5.5
DH3-CO2, bentonite, DH3-drillhole, 156.89 m (just below the middle of the Helvetiafjellet Formation, *c.* 25–30 m above the contact), Svalbard																
Z eu sp CA [1]	<1	>50	0.08	1.9	52.0	0.1582	0.0331	0.022226	0.000274	0.74	0.0516	0.0104	141.7	1.7	149	29
Z eu sp CA [1]	<1	>70	0.40	3.0	49.9	0.1689	0.0242	0.022012	0.000227	0.68	0.0557	0.0076	140.4	1.4	158	21
Z eu sp CA [1]	1	30	0.33	0.8	64.1	0.1335	0.0243	0.020416	0.000222	0.75	0.0474	0.0083	130.3	1.4	127	22
Z eu sp CA [1]	<1	>40	0.40	1.4	55.9	0.1418	0.0278	0.020167	0.000238	0.75	0.0510	0.0096	128.7	1.5	135	24
Z eu sp CA [1]	<1	>60	0.69	1.3	75.8	0.1460	0.0180	0.019823	0.000194	0.65	0.0534	0.0063	126.5	1.2	138	16
Z eu sp CA [1]	<1	>30	0.00	1.1	47.6	0.1254	0.0396	0.019720	0.000347	0.79	0.0461	0.0140	125.9	2.2	120	35
Z eu sp CA [1]	<1	>30	0.00	0.6	70.9	0.1437	0.0199	0.019534	0.000196	0.70	0.0534	0.0070	124.7	1.2	136	18
Z eu sp CA [1]	<1	>50	0.02	0.9	78.7	0.1288	0.0167	0.019380	0.000166	0.69	0.0482	0.0060	123.7	1.1	123	15
Z eu sp CA [1]	<1	>270	0.74	1.1	309.4	0.1283	0.0034	0.019340	0.000083	0.45	0.0481	0.0012	123.5	0.5	122.5	3.1
Z eu sp CA [1]	<1	>80	0.34	0.8	134.3	0.1315	0.0086	0.019327	0.000114	0.58	0.0493	0.0031	123.4	0.7	125.4	7.7
Z eu sp CA [1]	1	60	0.00	0.8	103.4	0.1280	0.0118	0.019249	0.000122	0.69	0.0482	0.0042	122.9	0.8	122	11
Z eu sp CA [1]	<1	>100	0.65	1.0	128.5	0.1327	0.0089	0.019236	0.000106	0.63	0.0500	0.0032	122.8	0.7	126.5	8.0
1893 (1893.6–1898.9 m), mafic sill, Severnaya borehole, Franz Josef Land, 64.411667, 81.149167																
B fr NA [12]	1	230	0.05	2.5	127.2	0.1317	0.0070	0.019070	0.000092	0.59	0.0501	0.0025	121.8	0.6	125.7	6.3
B bl NA [17]	1	990	0.15	3.0	413.7	0.1295	0.0018	0.019058	0.000095	0.50	0.0493	0.0006	121.7	0.6	123.6	1.7
B bl NA [17]	1	970	0.13	2.4	504.3	0.1273	0.0017	0.019007	0.000058	0.46	0.0486	0.0006	121.4	0.4	121.7	1.6
B bl NA [22]	1	950	0.09	10.2	128.2	0.1240	0.0039	0.018805	0.000116	0.28	0.0478	0.0014	120.1	0.7	118.7	3.5
1902 (1902.9 m), mafic sill, Severnaya borehole, Franz Josef Land, 64.411667, 81.149167																
Z tu CA [1]	<1	>1070	1.95	0.8	1639	0.1280	0.0010	0.019190	0.000079	0.64	0.0484	0.0003	122.5	0.5	122.3	0.9
Z eu CAr [1]	<1	>1280	2.41	1.1	1405	0.1244	0.0008	0.018509	0.000042	0.56	0.0487	0.0003	118.2	0.3	119.0	0.7
Z eu CAr [1]	<1	>45	1.77	0.4	133.4	0.1084	0.0104	0.017851	0.000215	0.46	0.0440	0.0040	114.1	1.4	104.5	9.5
1895 (1895.0 m), mafic sill, Severnaya borehole, Franz Josef Land, 64.411667, 81.149167																
Z fr lp tu CA [1]	<1	>220	1.84	1.0	289.7	0.1250	0.0041	0.019250	0.000074	0.52	0.0471	0.0015	122.9	0.5	119.6	3.7
Z fr lp CA [1]	<1	>1000	2.05	0.6	2081	0.1270	0.0007	0.019063	0.000048	0.64	0.0483	0.0002	121.7	0.3	121.4	0.6
Z eu CAr [1]	<1	>380	2.04	0.6	767.9	0.1260	0.0014	0.018999	0.000048	0.47	0.0481	0.0005	121.3	0.3	120.5	1.3
Z eu CAr [1]	<1	>760	3.77	1.0	905.2	0.1255	0.0012	0.018743	0.000049	0.49	0.0486	0.0004	119.7	0.3	120.1	1.1
Z eu CAr [1]	<1	>1130	2.47	0.6	2251	0.1251	0.0006	0.018716	0.000043	0.65	0.0485	0.0002	119.5	0.3	119.7	0.5
Z eu CAr [1]	<1	>660	1.88	0.5	1463	0.1247	0.0008	0.018666	0.000044	0.56	0.0484	0.0003	119.2	0.3	119.3	0.7
Z eu CAr [1]	<1	>440	1.72	0.7	730.5	0.1216	0.0013	0.018011	0.000042	0.49	0.0490	0.0005	115.1	0.3	116.6	1.2
2944 (2944.2–2947.6 m), mafic sill, Nagurskaya borehole, Franz Josef Land, 47.708333, 80.777778																
Z fr CAr [1]	<1	>55	0.30	1.4	66.4	0.1248	0.0198	0.019144	0.000173	0.72	0.0473	0.0072	122.2	1.1	119	18
Z tip CA [1]	<1	>80	0.39	0.8	132.5	0.1137	0.0082	0.017353	0.000102	0.61	0.0475	0.0033	110.9	0.6	109.3	7.4

[a]Z – zircon; B – baddeleyite; R – rutile; T – titanite; eu – euhedral; an – anhedral; lp – long prismatic ($l/w = >4$); sp – short prismatic; bl – thin blades; fr – fragments, broken prisms; tu – turbid; NA – not abraded; CA – chemical abrasion with overnight partial dissolution; CAr – chemical abrasion with only 2 hours partial dissolution; [1] number of grains in fractions

[b]Th/U model ratio inferred from $^{208}/^{206}$ ratio and age of sample

[c]Total amount of common Pb (initial + blank)

[d]Raw data corrected for fractionation

[e]Corrected for fractionation, spike, blank and initial common Pb; error calculated by propagating the main sources of uncertainty; initial common Pb corrected using Stacey & Kramers (1975) model compositions except for rutile and titanite in sample 7A that were corrected using the composition of co-existing pyroxene (6/4 = 18.821 ± 0.24 % and 7/4 = 15.662 ± 0.28 %); $^{206}Pb/^{238}U$ and $^{207}Pb/^{206}Pb$ values corrected for excess ^{206}Pb assuming Th/U = 4 for the parent magma and using the equation of Schärer (1984).

4.d. Sample DH3-CO2: bentonite in Helvetiafjellet Formation

Zircon in the bentonite occurs as a reasonably homogeneous population consisting principally of small, equant to short-prismatic crystals with a predominance of {100} and {101} crystal faces. The analyses yield a spread of ages, however, with two data points overlapping at about 140 Ma, another four in the range 130–126 Ma and a group of six overlapping and giving a weighted mean $^{206}Pb/^{238}U$ age of 123.3 ± 0.2 Ma (Fig. 4c). This coherent group is interpreted to indicate

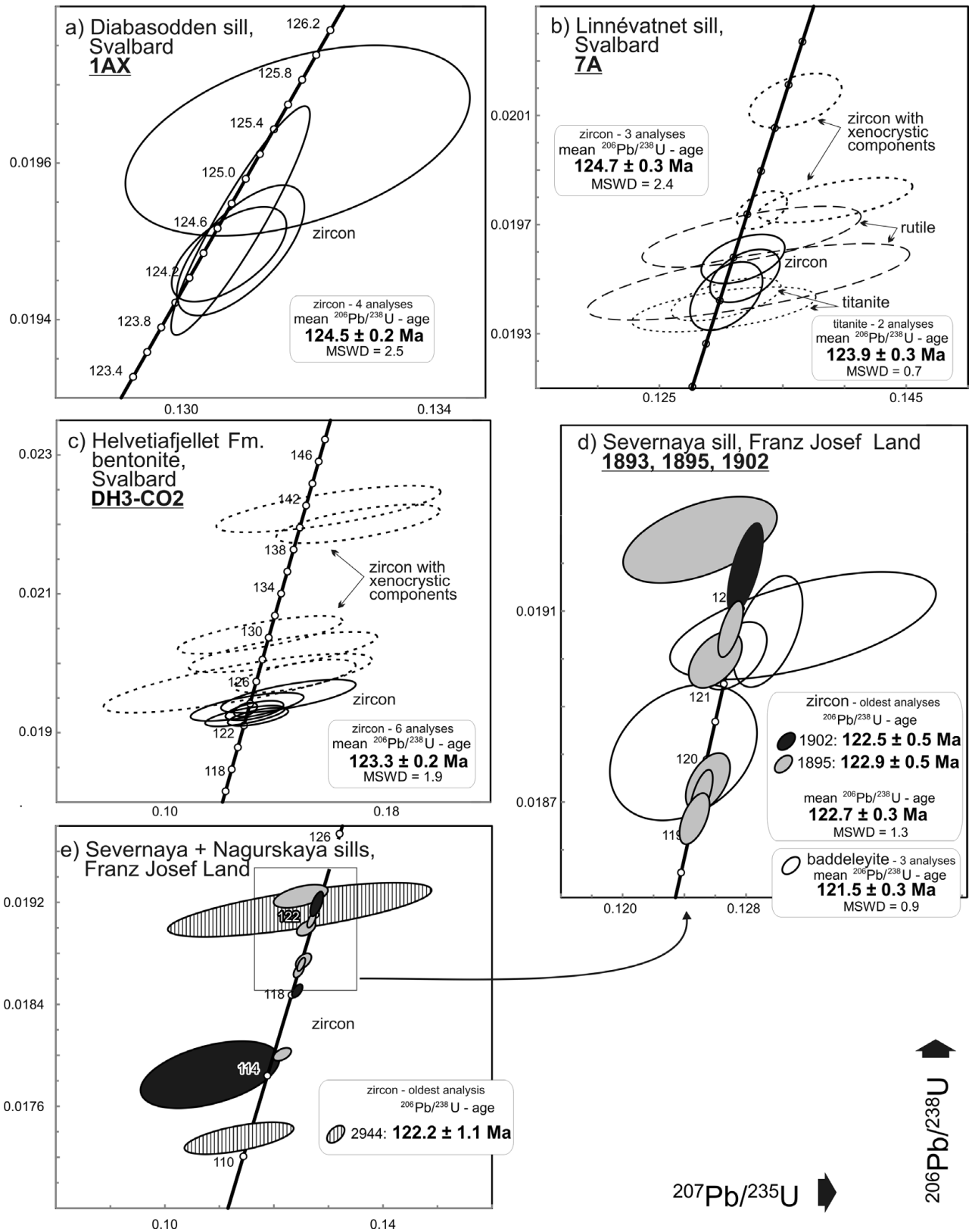

Figure 4. (a–d) Concordia diagrams showing U–Pb data for zircon, baddeleyite, titanite and rutile from mafic sills and bentonite from Svalbard and Franz Josef Land. Ellipses indicate the 2σ uncertainty.

the time of the volcanic event, whereas the older apparent dates likely reflect xenocrystic components either as cores or as entirely xenocrystic crystals formed during earlier magmatic phases.

4.e. Mafic sill, Severnaya borehole, Franz Josef Land

4.e.1. Sample 1893

Recovered zircon grains are mostly subrounded, frosted and heterogeneous, and likely of detrital origin. As the

sample integrated a 5 m section at the bottom of the sill (Fig. 3), the presence of detrital zircon probably reflects an imperfect separation of the mafic sill part of the core from the surrounding sediment. Two of the most euhedral 'magmatic-looking' zircons were dated, but these gave Cambrian and Mesoproterozoic ages (Table S1, Fig. S1 see online Supplementary Material available at http://journals.cambridge.org/geo). Analyses were therefore performed on baddeleyite, which occurs as 20–50 μm long, very thin blades. Three of the analyses overlap giving a weighted mean $^{206}Pb/^{238}U$ age of 121.5 ± 0.3 Ma. The fourth analysis is slightly younger (Fig. 4d).

Because of the small tabular nature of the baddeleyite crystals it was not possible to subject them to air abrasion (Krogh, 1982); the age must therefore be considered a minimum age. One effect that can be significant in such small tabular crystals is the loss of daughter nuclides due to alpha recoil. Davis & Davis (2010) observed that some loss is detectable in the outer 50 nm of baddeleyite crystals and the effect causes a reduction of the $^{206}Pb/^{238}U$ ratio by 20–30 % at 20 nm. If we assume that our baddeleyites are *c.* 5 μm thick, then about 2 % of their volume would have been affected by alpha recoil loss. This translates into a reduction of the Pb/U ratio by *c.* 0.25 %, corresponding to *c.* 0.4 Ma. The other potential effect, which is more difficult to quantify, is superimposed Pb loss by diffusion or alteration. For example, unabraded 55 Ma baddeleyite from mafic sills in the North Atlantic shows a reduction in the Pb/U ratio of 1–2 % with respect to coexisting zircon processed using abrasion (Svensen *et al*. 2010), whereas large baddeleyite from Karoo sills that was abraded gives the same age as zircon (Svensen *et al*. 2012). If we assume that baddeleyite in our sample 1893 lost 1–2 % by both alpha recoil and Pb diffusion, then its real age would have to be 1–2 Ma older, that is 122.5–123.5 Ma.

4.e.2. Samples 1895 and 1902

Some zircon grains with features typical of zircon in mafic rocks, i.e. resembling those described for sample 1AX, were recovered from samples 1895 and 1902 representing specific parts at the bottom of the Severnaya sill. Most of these grains were very metamict however, and first selections almost totally dissolved during the standard overnight partial dissolution procedure of the chemical abrasion process. Another batch of grains was subsequently only held in HF for a few hours in an attempt to preserve at least parts of the grains, but this short procedure did not manage to remove all the discordance and most of these analyses give too-young ages (Fig. 4d, e). The oldest analyses obtained from each sample give identical $^{206}Pb/^{238}U$ ages of 122.9 ± 0.5 and 122.5 ± 0.5 Ma, which combine into a weighted mean $^{206}Pb/^{238}U$ age of 122.7 ± 0.3 Ma. This age is consistent with the inference from the baddeleyite analyses and is considered a good estimate for the time of emplacement of the sill.

4.f. Sample 2944: mafic sill, Nagurskaya boreholes, Franz Josef Land

A few magmatic zircon crystals resembling those described above were also found in a sill from Nagurskaya. One of the analyses is discordant, but the second overlaps the oldest analyses from the Severnaya sill, giving a $^{206}Pb/^{238}U$ age of 122.2 ± 1.1 Ma (Fig. 4e). Their similarity suggests that the sills in Franz Josef Land are indeed 123–122 Ma.

4.g. Xenocrystic zircon in samples from mafic sills, Severnaya, Nagurskaya and Hooker Island boreholes, Franz Josef Land

Two of the samples discussed above (2944 and 1902) also contained older xenocrystic zircons giving ages of 308 Ma (2 grains) and *c.* 316 Ma (one grain, moderately discordant; Table S1, Fig. S1, online Supplementary Material available at http://journals.cambridge.org/geo). A grain with a similar but more discordant age was also found in sample 1852. Zircon in five other samples have Precambrian ages ranging from 3100 to 750 Ma, some concordant and some highly discordant (Fig. S1). Sharply euhedral prisms from a sample from Hooker Island yield instead a Triassic, two Permian and a Carboniferous age. The provenance of these grains is not understood.

5. Discussion

5.a. Timing of magmatism in Svalbard and Franz Josef Land

The new results confirm the stratigraphic evidence for a predominant Early Cretaceous (Barremian) age of mafic magmatism in Svalbard with overlapping ages of 124.5 ± 0.2 and 124.7 ± 0.3 Ma for the two large sills in Svalbard and a 1.5 Ma younger age for the felsic tuff in the Helvetiafjellet Formation. The sills on Franz Josef Land are somewhat younger as indicated by the age of the Severnaya sill at 122.7 ± 0.3 Ma and the single result of 122.2 ±1.1 Ma for a sill on Nagurskaya Island. Taken together, the new U–Pb ages show that these episodes of magmatic activity lasted for at least a few million years, which is consistent with the presence of multiple extrusive horizons in the Cretaceous stratigraphic record.

The new U–Pb ages, together with the confined stratigraphic interval of the lava flows, suggest that the magmatic episode was likely restricted in time and did not span as much of the Mesozoic as suggested by the previously published K–Ar and Ar–Ar data. In fact, some of the contrasting values provided by these dating methods on some of the same bodies dated here by U–Pb (Nejbert *et al*. 2011; S. Polteau, unpub. data, 2011) prove that the Ar systems in several cases have been severely reset by secondary events. The

geological reasons for the isotopic disturbances are not straightforward. Our sample 7A was affected by very intense alteration which transformed the plagioclase in particular and also, to various degrees, the other minerals. The growth of rutile and titanite appears to be the expression of different stages of this alteration. The fact that rutile yields the same age as coexisting magmatic zircon shows that this specific alteration event, likely related to the local breakdown of pyroxene, occurred immediately after emplacement of the unit, probably as a response to the fluids activated in the contact metamorphic aureole. Titanite does not appear to be associated with or derived from rutile and was likely produced by some other reaction, although in thin section the link is difficult to establish. The up to 1 Ma younger age of the titanite supports its formation by a distinct reaction, presumably as a response to late fluid activity promoted by subsequent magmatic pulses. Interestingly, none of these minerals were affected by the younger disturbances recorded in the K–Ar systems, such as the K–Ar ages of 92 and 81 Ma reported for the Diasbasodden sill (Nejbert *et al*. 2011) showing that the latter were likely affected by other weak and very local effects. Unless confirmed by independent evidence, the significance of the Ar ages therefore remains the subject of some uncertainty.

5.b. HALIP magmatism in the Arctic context

In light of the above considerations it is evident that some of the chronologic evidence used to formulate correlations and propose specific processes associated with the opening of the Arctic oceanic basins is problematic. Some of the chronology is based on fairly solid U–Pb results, such as the *c.* 90 Ma ages of the Hansen Point volcanics and the Wootton Intrusion in northern Ellesmere Island (Trettin & Parrish, 1987) or the 70–60 Ma Kap Washington Suite in northern Greenland (Thorarinsson *et al*. 2011). Other chronological evidence is more uncertain and should be verified by more robust dating methods. The present study suggests that HALIP consists of one volcanic province in the Barents Sea (BLIP) that is older by *c.* 40 Ma, but overlaps in geographic distribution with the younger volcanic event dominating the Canadian Arctic. The study further shows that it is possible to find units and minerals datable by U–Pb by applying informed and systematic search criteria. The new U–Pb ages, together with the confined stratigraphic interval of the lava flows, suggest that the magmatic episode was likely restricted in time and did not span as much of the Mesozoic as suggested by the K–Ar and Ar–Ar data.

Acknowledgments. We acknowledge a Petrobar grant to Sverre Plancke. Ivar Midtkandal and Ellen Eckhoff-Planke are thanked for their assistance in Svalbard during field work and collection of samples. The UNIS CO2 Lab kindly allowed the sampling of the tuff from the BH3 borehole and Snorre Olaussen and Alvar Braathen (UNIS) helped with the sampling. We are also grateful to NPD for their support and the Laboratory of Mineralogical and Fission Track Analysis of the Geological Institute, Russian Academy who carefully extracted zircon and baddeleyite from the samples from Franz Josef Land. Finally, we thank Sandra Kamo and an anonymous reviewer for constructive reviews.

References

ALVEY, A., GAINA, C., KUSZNIR, N. J. & TORSVIK, T. H. 2008. Integrated crustal thickness mapping and plate reconstructions for the high Arctic. *Earth and Planetary Science Letters* **274**, 310–21.

AMUNDSEN, H., EVDOKIMOV, A., DIBNER, V. & ANDRESEN, A. 1998. Petrogenic significance and evolution of Mesozoic magmatism, Franz Josef Land, northeastern Barents Sea. In *Geological Aspects of Franz Josef Land and the Northernmost Barents Sea. The Northern Barents Sea Geotraverse* (eds Solheim, A., Musatov, E. & Heintz, N.) pp. 105–20. Norsk Polarinstitutt Meddelelser 151.

BUCHAN, K. L. & ERNST, R. E. 2006. Giant dyke swarms and the reconstruction of the Canadian Arctic islands, Greenland, Svalbard, and Franz Josef Land. In *Dyke Swarms—Time Markers of Crustal Evolution* (eds Hanski, E., Mertanen, S., Rämö, T. & Vuollo, J.), pp. 27–48. Taylor & Francis, London, UK.

CHARLES, A. J., CONDON, D. J., HARDING, I. C., PÄLIKE, H., MARSHALL, J. E. A., CUI, Y., KUMP, L. & CROUDACE, I. W. 2011. Constraints on the numerical age of the Paleocene-Eocene boundary. *Geochemistry Geophysics Geosystems* **12**, Q0AA17, doi:10.1029/2010GC003426.

CORFU, F. 2004. U-Pb age, setting, and tectonic significance of the anorthosite-mangerite-charnockite-granite-suite, Lofoten-Vesterålen, Norway. *Journal of Petrology* **45**, 1799–819.

DAVIS, W. J. & DAVIS, D. W. 2010. Alpha recoil loss from baddeleyite evaluated by depth profiling and numerical modelling: implications for U-Pb ages. *Goldschmidt Conference Abstracts*, *Geochimica et Cosmochimica Acta* **74**(11), A213.

DIBNER, V. D. (ed.) 1998. *Geology of Franz Jozef Land*. Norsk Polarinstitutt, Meddelelser **146**, 190 p.

DYPVIK, H., FJELLSÅ, B., PCELINA, T. M., SOKOLOV, A & RÅHEIM, A. 1998. The diagenetic of the Triassic succession of Franz Josef Land. In *Geological Aspects of Franz Josef Land and the Northernmost Barents Sea. The Northern Barents Sea Geotraverse* (eds Solheim, A., Musatov, E. & Heintz, N.), pp. 83–104. Norsk Polarinstitutt Meddelelser 151.

ERNST, R. & BLEEKER, W. 2010. Large igneous provinces (LIPs), giant dyke swarms, and mantle plumes: significance for breakup events within Canada and adjacent regions from 2.5 Ga to the Present. *Canadian Journal of Earth Sciences* **47**, 695–739.

FALEIDE, J. I., TSIKALAS, F., BREIVIK, A. J., MJELDE, R., RITZMANN, O., ENGEN, Ø., WILSON, J. & ELDHOLM, O. 2008. Structure and evolution of the continental margin off Norway and the Barents Sea. *Episodes* **31**, 82–91.

GRACHEV, A. F. 2000. Mantle plumes and the problems of Geodynamics. *Isvestiya, Physics of the Solid Earth* **36**, 263–94.

GRACHEV, A. F., ARAKELYANTZ, M. M., LEBEDEV, V. A., MUSATOV, E. E. & STOLBOV, N. M. 2001. New K-Ar ages for basalts from Franz Josef Land. *Russian Journal of Earth Sciences* **3**, 79–82.

GROGAN, P., NYBERG, K., FOTLAND, B., MYKLEBUST, R., DAHLGREN, S. & RIIS, F. 2000. Cretaceous magmatism south and east of Svalbard: evidence from seismic

reflection and magnetic data. *Polarforschung* **68**, 25–34.

HARLAND, W. B, LESTER, M., ANDERSON, L. M. & MANASRAH, D. (eds) 1997. *The Geology of Svalbard*. Geological Society, London, Memoirs **17**.

JAFFEY, A. H., FLYNN, K. F., GLENDENIN, L. E., BENTLEY, W. C. & ESSLING, A. M. 1971. Precision measurement of half–lives and specific activities of ^{235}U and ^{238}U. *Physical Review, Section C, Nuclear Physics* **4**, 1889–906.

KROGH, T. E. 1973. A low contamination method for hydrothermal decomposition of zircon and extraction of U and Pb for isotopic age determinations. *Geochimica et Cosmochimica Acta* **37**, 485–94.

KROGH, T. E. 1982. Improved accuracy of U–Pb zircon ages by the creation of more concordant systems using an air abrasion technique. *Geochimica et Cosmochimica Acta* **46**, 637–49.

LEVSKII, L. K., STOLBOV, N. M., BOGOMOLOV, E. S., VASIL'EVA, I. M. & MAKAR'EVA, E. M. 2006. Sr–Nd–Pb isotopic systems in basalts of the Franz Josef Land archipelago. *Geochemistry International* **44**, 327–37.

LUDWIG, K. R. 2009. Isoplot 4.1. A geochronological toolkit for Microsoft Excel. *Berkeley Geochronology Center Special Publication* **4**, 76.

MAHER, H. D. 2001. Manifestations of Cretaceous High Arctic large igneous province in Svalbard. *Journal of Geology* **109**, 91–104.

MATTINSON, J. M. 2010. Analysis of the relative decay constants of ^{235}U and ^{238}U by multi-step CA-TIMS measurements of closed-system natural zircon samples. *Chemical Geology* **275**, 186–98.

MINAKOV, A., MJELDE, R., FALEIDE, J. I., FLUEH, E. R., DANNOWSKI, A. & KEERS, H. 2012. Mafic intrusions east of Svalbard imaged by active-source seismic tomography. *Tectonophysics* **518–521**, 106–18.

NEJBERT, K., KRAJEWSKI, K. P., DUBINSKA, E. & PECSKAY, Z. 2011. Dolerites of Svalbard, north-west Barents Sea Shelf: age, tectonic setting and significance for geotectonic interpretation of the High-Arctic Large Igneous Province. *Polar Research* **30**, 7306, doi: 10.3402/polar.v30i0.7306.

PISKAREV, A. L., HEUNEMANN, CH., MAKAR'EV, A. A., MAKAR'EVA, E. M., BACHTADSE, V. & ALEKSYUTIN, M. 2009. Magnetic parameters and variations in the composition of magmatic rocks from the Franz Josef Land archipelago. *Physics of the Earth* **2**, 66–83.

SCHÄRER, U. 1984. The effect of initial ^{230}Th disequilibrium on young U-Pb ages: the Makalu case, Himalaya. *Earth and Planetary Science Letters* **67**, 191–204.

SOLHEIM, A., MUSATOV, E. E., HEINTZ, N. & ELVERHØI, A. 1998. Geological evolution and correlation between Franz Josef Land and Svalbard. The Northern Barents Sea Geotraverse: introduction to the project. In *Geological Aspects of Franz Josef Land and the Northernmost Barents Sea. The Northern Barents Sea Geotraverse* (eds Solheim, A., Musatov, E. & Heintz, N.), pp. 5–9. Norsk Polarinstitutt Meddelelser 151.

STACEY, J. S. & KRAMERS, J. D. 1975. Approximation of terrestrial lead isotope evolution using a two-stage model. *Earth and Planetary Science Letters* **26**, 221–97.

SVENSEN, H., PLANKE, S. & CORFU, F. 2010. Zircon dating ties Northeast Atlantic sill emplacement to initial Eocene global warming. *Journal of the Geological Society, London* **167**, 433–6.

SVENSEN, H., CORFU, F., POLTEAU, S., HAMMER, Ø. & PLANKE, S. 2012. Rapid Magma Emplacement in the Karoo Large Igneous Province. *Earth and Planetary Science Letters* **325–326**, 1–9.

TARAKHOVSKY, A. N., FISHMAN, M. V., SHKOLA, I. V. & ANDREICHEV, V. L. 1983. The age of the traps of the Fanz Josef Land. In *Prediction and Estimation of the Nickel Content of New Metalliferous Areas on the Northern Part of the Siberian Platform* (ed. Kavardin, G. I.), Sevmorgeologia, Leningrad (in Russian), pp. 100–8.

THORARINSSON, S. B., HOLM, P. M., TAPPE, S., HEAMAN, L. M. & TEGNER, C. 2011. Late Cretaceous–Palaeocene continental rifting in the High Arctic: U–Pb geochronology of the Kap Washington Group volcanic sequence, North Greenland. *Journal of the Geological Society, London* **168**, 1093–106.

TRETTIN, H. P. & PARRISH, R. 1987. Late Cretaceous bimodal magmatism, northern Ellesmere Island: isotopic age and origin. *Canadian Journal of Earth Sciences* **24**, 257–65.

WORSLEY, D. 2008. The post-Caledonian development of Svalbard and the western Barents Sea. *Polar Research* **27**, 298–317.